To the Graduate Council:

I am submitting herewith a dissertation written by Xiaochun He entitled "Multiplicity Dependence of Bose-Einstein Correlation and Quantum Statistics." I have examined the final copy of this dissertation for form and content and recommend that it be accepted in partial fulfillment of the requirements for the degree of Doctor of Philosophy, with a major in Physics.

C. C. Shih

C. C. Shih, Major Professor

We have read this dissertation
and recommend its acceptance:

Edward R Harris

Edward J. Hart

John E. Bloor

Accepted for the Council:

Linda Mitchell

Vice Provost
and Dean of The Graduate School

MULTIPLICITY DEPENDENCE OF BOSE-EINSTEIN CORRELATION AND QUANTUM STATISTICS

A Dissertation
Presented for the
Doctor of Philosophy
Degree
The University of Tennessee, Knoxville

Xiaochun He
May 1991

ACKNOWLEDGEMENTS

Prof. C. C. Shih has provided me with invaluable guidance, encouragement, and support through every step of this research. For his unfailing confidence in me, I am honored and deeply grateful. I appreciate and thank others who served on my committee: Prof. E. G. Harris, Prof. E. Hart, and Prof. J. E. Bloor.

I thank my former academic adviser, Prof. Jingye Zhang, and his family for their endless encouragement, support, and friendship.

DEDICATION

To my parents: Deng-Qin He, Hong-Zhai Dou

献给我敬爱的父母亲

贺登勤，窦红寨

ABSTRACT

The use of a multiplicity cut introduces a bias which distorts the Bose-Einstein correlation of a quantum statistical formalism, and this reveals that the bias has a substantial effect on the estimate of the true correlation length and chaoticity. It also reveals a strong antibunching effect at a fixed event multiplicity, as has been observed experimentally.

TABLE OF CONTENTS

CHAPTER		PAGE
1. Introduction		**1**
1.1	Historical review of Bose-Einstein correlations	1
1.2	The motivation of the current study	4
1.3	The quantum statistical approach	5
2. Bose-Einstein Correlation Formalism		**8**
2.1	Single and double inclusive distributions	8
2.2	Density operator and coherent state P-representation	10
3. Quantum Correlations and Multiplicity Dependences		**13**
3.1	Correlation in rapidity	13
3.2	Single domain	16
3.2.1	Field operator and its P-representation	17
3.2.2	Multiplicity distributions	18
3.2.3	Lorentzian profile	20
3.3	Multiple domains	21
4. Monte Carlo Simulation		**24**

CHAPTER PAGE

4.1 Monte Carlo formalism 24

4.2 Numerical results 27

4.3 Conclusions 33

5. Summary 36

BIBLIOGRAPHY 38

APPENDIX 40

A. Eigenvalues and eigenfunctions 41

B. Monte Carlo flow chart 44

VITA 45

LIST OF FIGURES

FIGURE **PAGE**

3.1 Multi domains in rapidity 23

4.1 Five domains in rapidity 25

4.2 Comparison of $C_{(2)}$ for the partially coherent case 28

4.3 Comparison of $C_{(2)}$ for the fully chaotic case 29

4.4 Multiplicity dependence of $C_{(2)}$ 30

CHAPTER 1

Introduction

1.1 Historical review of Bose-Einstein correlations

Bose-Einstein correlation (BEC) has its origins in astrophysics where the technique of intensity interferometry was first used. The intensity interferometry method was developed by Hanbury-Brown and Twiss in the 1950's, as a means of determining the dimensions of distant astronomical objects[1]. The method of intensity interferometry is now commonly referred to as Hanbury-Brown and Twiss (HBT) effect.

Historically, inspired by HBT effect, the first observation of Bose-Einstein correlations in elementary-particle collisions was made by Goldhaber et al. in 1959. They studied the intensity correlation in multi-particle production of the 1.05 GeV/c anti-proton annihilation in a bubble chamber. Goldhaber, Goldhaber, Lee, and Pais (GGLP) interpreted the angular correlations among pions within the context of a statistical model in which the particle production was confined within a region of spatial dimension of the order 1 fm in 1960[2]. GGLP have also shown that like-charge pions with small relative momenta are emitted with enhanced

probability as compared to unlike-charge pions. Following GGLP, many of the experiments performed on two-pion correlations during the 1960's and early 1970's either determined the parameters of the GGLP statistical formalism or used the GGLP model to deduce source volumes[3] (Xuong and Lynch, 1962; Bartke et al., 1967; Donald et al., 1969; De Baere et al., 1970; Boesebeck et al., 1973; Oh et al., 1975).

Kopylov and Podgoretskii (1972, 1973) developed a convenient formalism for interpreting two-particle correlation measurements in terms of the space-time extent of the particle-emitting source region. Subsequent to this development, a sizable number of particle physics experiments were performed and interpreted in terms of the source geometry[3]. For example, experiments involving the hadron-hadron collisions are: Biswas et al., 1976; Borreani et al., 1976; Calligarich et al., 1976; Deutschmann et al., 1976, 1982; Grard et al., 1976; Angelini et al., 1977; Angelov et al., 1977, 1981; Ezell et al., 1977; Cooper et al., 1978; De Wolf et al., 1978; Goossens et al., 1978; Loktionov et al., 1978; Drijard et al., 1979; Akesson et al., 1983, 1985, 1987; Breakstone et al., 1985, 1987; Adamus et al., 1988; Albajar et al., 1989. Experiments involving lepton-hadron collisions are: Arneodo et al., 1986; and Allasia et al., 1988. And experiments involving lepton-lepton collisions are: Aihara et al., 1985; Althoff et al., 1985, 1986; Avery et al., 1985; and Juricic et al., 1989.

Following these experiments, several models are used for parameterizations of particle emission. The two most commonly used parameterizations are: (1) the Gaussian source distribution (Goldhaber, et al., 1960; Koonin, 1977; Yano and Koonin, 1978; Lednicky and Podgoretskii, 1979; Kvatadze, Moller, and Lorstad, 1988; Capella and Krzywicki, 1989), and (2) the radiation from a sphere or disk, often referred to as the Kopylov-Podgoretskii parametrization (Kopylov and Podgoretskii, 1972, 1973; Cocconi, 1974; Kopylov, 1974; Podgoretskii and Cheplakov, 1986). These two distributions represent time-invariant sources moving with uniform velocity. Models based on expanding sources are also discussed by some authors (Pratt, 1984, 1986; Kolehmainen and Gyulassy, 1986; Averchenkov, Makhlin, and Sinyukov, 1987; Machlin and Sinyyukov, 1987; Hama and Padula, 1988). The formalisms for the correlation function based upon the string model (Bowler, 1985, 1987; Andersson and Hofmann, 1986), and other statistical and dynamical models have also appeared in literature[3].

The above analyses have been performed with several different source parametrizations. The dimensions determined through the correlation lengths were performed in various variable spaces, such as the 4-momentum-transfer square, the transverse momentum difference, or the rapidity difference[4]. However, it is often difficult to compare results from different experiments because of differences in analysis methods. The extracted parameters are very sensitive to the method of analysis

and to the experimental approach used.

1.2 The motivation of the current study

The motivation of the current study comes from the study of the deconfined quantum chromodynamics (QCD) state, i.e., quark gluon plasma (QGP). In recent years, this study has attracted renewed interest in BEC, in an attempt to estimate the dimensions of the region in which a new phase of matter, QGP, most likely exists at the extreme conditions in relativistic heavy-ion collisions. It is generally believed that when the created energy density within the interacting region increases sufficiently, the hadronic matter becomes deconfined and forms a QGP phase of matter. However, there are no definite conclusions about the conditions under which the QGP could exist.

In order to reach a QGP phase, one uses relativistic heavy-ion collisions as a basic tool to create an exotic state of high energy density. An accurate estimation of the energy density and temperature created in a high energy collision, such as the future RHIC facility at Brookhaven National Laboratory is essential for assessing the existence of QGP. However, experimental limitations and some dynamic considerations suggest the necessity of using experimental triggers in the measurements, such as a cut in the lowest transverse momentum, the transverse

energy, phase space, or multiplicity, etc. Different experimental triggers will be very important in the determination of whether a QGP phase is created for central collisions or not. The research of this dissertation is to study how the BEC could be affected when the multiplicity bias (cut) is used in a quantum statistical (QS) approach. This effect must be clarified if the multiplicity bias is to be introduced as an effective diagnostic tool in the BEC study, before any assessment of the size and lifetime of the QGP can be made.

1.3 The quantum statistical approach

The quantum statistical approach in particle physics was proposed first by Giovannini (1973) and Suzuki (1974), and fully examined by Suger et al. (1974), Gyulassy (1979), Fowler and Weiner (1978,1984) and Shih (1984). This approach shares the same background as quantum optics (QO), where Glauber, Klauder, Mandal, Jaiswal and Mehta developed a successful quantum optical theory in the 1960's and 1970's. In both the areas of QO and the particle physics research, coherent states are introduced to analyze the probability of the particle statistics. Both the electromagnetic field in QO and the pion field in particle physics are treated as a superposition of two components: one coherent, and the other chaotic. With this approach, hadronic multiplicity distributions in high energy

collisions can be successfully analyzed[5,6]. QS is also successful in dealing with particle correlations, such as in BEC[7]. One of the most important roles of our QS approach is that it automatically relates the BEC with the particle multiplicity distribution and allows us to study the BEC with the multiplicity biases.

In the QS model, the underlying quantum fields and the number operator for the particles do not commute. The formalism for the BEC, as well as the multiplicity distributions provided by QS are expressed in terms of fields, where the ensemble averages are performed with the help of the density matrix ρ. This means that measurements of "true" BEC can be performed only when no restriction is made on the multiplicity n, which fluctuates from event to event. In practice, however, very often such restrictions are imposed, either for technical reasons or because of theoretical prejudices. Thus, for example, one sometimes argues that by selecting events with $n \geq n_{min}$, where n_{min} is in general an energy-dependent quantity, one gets, through BEC, information about the interesting "central" collisions. This selection, which hitherto has always been done in terms of *charged* particles only, introduces (indirectly, i.e. via the obvious correlation between the charged and, say, negative particle multiplicities in a given event) a bias in BEC measurements. It turns out from the study below that the magnitude of this effect is (especially at low multiplicity n) surprisingly large and must not be ignored.

This thesis is organized as follows: The general definition of BEC as the ratio of

a double inclusive distribution with respect to the product of two single inclusive distributions is given in Chapter 2. A brief introduction to the method of using the density operator and P-representation to calculate BEC is also given in Chapter 2. In Chapter 3, we will introduce a simple quantum statistical model to analyze BEC in rapidity space. A Monte Carlo simulation and the numerical results are given in Chapter 4. Summary of the study is given in Chapter 5. Two appendices follow Chapter 5. Appendix A outlines the eigenvalue solution of this QS model, Appendix B gives the Monte Carlo flow chart.

CHAPTER 2

Bose-Einstein Correlation Formalism

2.1 Single and double inclusive distributions

The study of Bose-Einstein correlation (BEC) involves the search for the correlations between two identical bosonic particles (e.g. $\pi^-\pi^-$, $\pi^+\pi^+$, ...) produced in high energy hadronic collisions. In this study we will concentrate only on pions with negative charge. Unless specified explicitly, all particles considered are taken to be negative pions. We start with the Bose-Einstein correlation given by[2,8]

$$C_{(2)}(\vec{q}_1, \vec{q}_2) = \frac{P_2(\vec{q}_1, \vec{q}_2)}{P_1(\vec{q}_1)P_1(\vec{q}_2)}, \tag{2.1}$$

where

$$P_2(\vec{q}_1, \vec{q}_2) = \frac{1}{\sigma}\frac{d^6\sigma(\vec{q}_1, \vec{q}_2)}{d^3q_1 d^3q_2}, \tag{2.2}$$

$$P_1(\vec{q}) = \frac{1}{\sigma}\frac{d^3\sigma(\vec{q})}{d^3q}. \tag{2.3}$$

Here $P_1(\vec{q})$ and $P_2(\vec{q}_1, \vec{q}_2)$ are the single inclusive and double inclusive pion distributions[8]. From these definitions, $P_1(\vec{q})$ and $P_2(\vec{q}_1, \vec{q}_2)$ are related to

$$\int d^3q P_1(\vec{q}) = \overline{n}, \tag{2.4}$$

and

$$\int d^3q_1 d^3q_2 P_2(\vec{q}_1, \vec{q}_2) = \overline{n(n-1)}, \tag{2.5}$$

where $\overline{n}$ is the averaged pion multiplicity, and $\overline{n(n-1)}$ is the averaged number of pion pairs. It is apparent that when two pions are not correlated, $C_{(2)}(\vec{q}_1, \vec{q}_2) = 1$, regardless of the form of the individual pion multiplicity distribution.

Given a final state ϕ_j, the single pion inclusive distribution for momentum $\vec{q}$ is given by[8,9],

$$\begin{aligned} P_1(\vec{q}) &= \sum_X | < X|a(\vec{q})|\phi_j > |^2 \\ &= < \phi_j|a^\dagger(\vec{q})a(\vec{q})|\phi_j > \\ &= < \phi_j|N(\vec{q})|\phi_j > \end{aligned} \tag{2.6}$$

where the summation is over a complete basis of the final state configuration $|X>$. $a^\dagger(\vec{q})$ and $N(\vec{q}) = a^\dagger(\vec{q})a(\vec{q})$ are the pion creation and number density operators for pions of momentum $\vec{q}$. Eq.(2.6) is generalized for a more general quantum statistical ensemble in terms of a density operator ρ given by

$$\rho = \sum_{j,k} p_{jk}|\phi_j >< \phi_k|, \tag{2.7}$$

where p_{jk} are constants characterizing the relative contributions from different states $\{|\phi_j>\}$ in the ensemble. Eq.(2.6) is then replaced by

$$P_1(\vec{q}) = Tr\{\rho N(\vec{q})\}. \tag{2.8}$$

Thus $P_1(\vec{q})$ is just the average pion number density with momentum $\vec{q}$. Similarly, the double inclusive distribution, $P_2(\vec{q}_1, \vec{q}_2)$, is given in terms of the density operator ρ by

$$\begin{aligned} P_2(\vec{q}_1, \vec{q}_2) &= \sum_X | < X | a(\vec{q}_1) a(\vec{q}_2) | \phi_j > |^2 \\ &= < \phi_j | a^\dagger(\vec{q}_1) a^\dagger(\vec{q}_2) a(\vec{q}_2) a(\vec{q}_1) | \phi_j > \\ &= Tr\{\rho a^\dagger(\vec{q}_1) a^\dagger(\vec{q}_2) a(\vec{q}_2) a(\vec{q}_1)\}. \end{aligned} \tag{2.9}$$

$P_2(\vec{q}_1, \vec{q}_2)$ is obviously the average density of the pion pairs with momentum $\vec{q}_1$ and $\vec{q}_2$.

In practice, ρ is very complicated and can not be calculated exactly, since it requires the ensemble of complete solutions of the coupled hadronic field equations. It is therefore necessary to introduce phenomenological parametrizations for ρ. In the following sections the parameterization of ρ is furnished through a coherent state P-representation.

2.2 Density operator and coherent state P-representation

Simple phenomenological parametrizations can provide useful guidelines for the production dynamics in the absence of a fundamental theory of strong interaction dynamics. In hadronic physics, similar to the study of quantum optics, a wide class of density operators can be written in diagonal form in the coherent state

representation[8,10,11].

We start with a coherent state $|\alpha_1>$, the eigenstate of the destruction operator $a(\vec{q}_1)$, given by

$$a(\vec{q}_1)|\alpha_1>=\alpha_1(\vec{q}_1)|\alpha_1>\,. \tag{2.10}$$

In a so called P-representation, the density matrix ρ projected into the space of fixed $\vec{q}_1$ is written as

$$\rho_1=\int d^2\alpha_1\mathcal{P}_1(\alpha_1)|\alpha_1><\alpha_1|, \tag{2.11}$$

with

$$\int d^2\alpha_1=\int dRe(\alpha_1)\int dIm(\alpha_1).$$

Here $\mathcal{P}_1(\alpha_1)$ is a real-valued weighting function giving the quasi-probability distribution of the state $|\alpha_1>$. With this representation, Eq.(2.8) becomes

$$\begin{aligned} P_1(\vec{q}_1) &= \int d^2\alpha_1 <\alpha_1|\mathcal{P}_1(\alpha_1)a^\dagger(\vec{q}_1)a(\vec{q}_1)|\alpha_1> \\ &= \int d^2\alpha_1\mathcal{P}_1(\alpha_1)|\alpha_1(\vec{q}_1)|^2. \end{aligned} \tag{2.12}$$

Similarly, the density operator ρ projected into the joint space of fixed $\vec{q}_1$ and fixed $\vec{q}_2$ is written as

$$\rho_2=\int d^2\alpha_1\int d^2\alpha_2\mathcal{P}_2(\alpha_1,\alpha_2)|\alpha_1,\alpha_2><\alpha_1,\alpha_2|, \tag{2.13}$$

and Eq.(2.9) becomes

$$P_2(\vec{q}_1,\vec{q}_2)=\int d^2\alpha_1(\vec{q}_1)\int d^2\alpha_2(\vec{q}_2)\mathcal{P}_2(\alpha_1(\vec{q}_1),\alpha_2(\vec{q}_2))|\alpha_1(\vec{q}_1)|^2|\alpha_2(\vec{q}_2)|^2. \tag{2.14}$$

We notice that once $\mathcal{P}_1(\alpha_1(\vec{q}_1))$ in Eq.(2.12) and $\mathcal{P}_2(\alpha_1(\vec{q}_1), \alpha_2(\vec{q}_2))$ in Eq.(2.14) are specified, $C_{(2)}(\vec{q}_1, \vec{q}_2)$ can be evaluated directly by using Eq.(2.1).

Practically, the correlation function $C_{(2)}(\vec{q}_1, \vec{q}_2)$ is rarely calculated fully in its 6-dimensional form according to Eq.(2.1). Instead, the actual correlation function is projected into lower dimensions, e.g., transverse momentum difference of the two pions[12], or the rapidity difference $y_g = |y_1 - y_2|$[13]. Here the rapidity y of a particle is defined by

$$y = \frac{1}{2} \, ln \frac{E + q_L}{E - q_L}, \tag{2.15}$$

where E and q_L are the energy and the logitudinal momentum of the particle being detected. The main reason for choosing this variable is that the invariant single inclusive cross section $(d\sigma/dy)$ for high energy multi-particle production processes is known to be a slowly varying function of y in the central region. This regularity of the cross section is often referred to as the "central plateau"[14]. In the following study, we shall analyze the BEC in the rapidity space.

CHAPTER 3

Quantum Correlations and Multiplicity Dependences

3.1 Correlation in rapidity

Using rapidity y as the variable for the BEC analysis in the central region, the destruction operator $a(\vec{q})$ is naturally replaced by a pion field operator $\pi(y)$. We further assume that the pion field $\pi(y)$ is a superposition of a coherent component and a chaotic one expressed as

$$\pi(y) = \pi_{coh}(y) + \pi_{chao}(y). \tag{3.1}$$

Here the coherent field $\pi_{coh}(y)$ is chosen to be

$$\pi_{coh}(y) = \pi_{coh,0} e^{-iw_{coh}y}, \tag{3.2}$$

where $\pi_{coh,0}$ is a constant. w_{coh} is the "frequency" (monochromatic) of the coherent signal, and is the boost variable conjugate to y[14].

The random field $\pi_{chao}(y)$ is realized in a complex Gaussian ensemble by its two lowest moments

$$< \pi_{chao}(y) >_{ensemble} = 0, \tag{3.3}$$

and

$$<\pi^*_{chao}(y_1)\pi_{chao}(y_2)>=\Gamma(y_1,y_2). \tag{3.4}$$

All the higher order field correlation functions can then be expressed by the second order field correlation function $\Gamma(y_1,y_2)$ through a proper reduction procedure. We start with

$$\pi_{chao}(y)=\tilde{\pi}_{chao}(y)e^{-iw_{chao}y}, \tag{3.5}$$

where w_{chao} is the central "frequency" of the chaotic field. In the present study, for the sake of simplicity, we shall assume that, as is customary in optics[15], $w_{chao}=w_{coh}$.

Given Eq.(3.5), the correlation function Eq.(3.4) can be renormalized and written as

$$\Gamma(y_1,y_2)=\Gamma_0 e^{-iw_{chao}(y_2-y_1)}\gamma(y_1,y_2), \tag{3.6}$$

with $\Gamma_0=\Gamma(0,0)$, and $\gamma(0,0)=1$. So that the constant Γ_0 is related to the mean numbers of particles, $\overline{n}_{chao}$, from the chaotic component. That is, for a given rapidity domain Δy,

$$\overline{n}_{chao}=\Delta y\,\Gamma_0. \tag{3.7}$$

Adding $\overline{n}_{chao}$ to the mean numbers of particles, $\overline{n}_{coh}$, from the coherent component given by

$$\overline{n}_{coh}=\Delta y\,|\pi_{coh,0}|^2, \tag{3.8}$$

we get the total mean numbers of particles $\overline{n}$

$$\overline{n} = \overline{n}_{chao} + \overline{n}_{coh}. \tag{3.9}$$

The relative strength of the two components of the pion field $\pi(y)$ can be specified by a chaoticity parameter p, defined by

$$\begin{aligned} p &= \frac{\overline{n}_{chao}}{\overline{n}} \\ &= \frac{\Gamma_0}{\Gamma_0 + |\pi_{coh,0}|^2}. \end{aligned} \tag{3.10}$$

In the absence of a multiplicity bias, the above formalism of partially coherence leads to a specific form of $C_{(2)}(y_1, y_2)$[6] in BEC. The single and double inclusive distributions (Eqs.(2.12) and (2.14)) are given by

$$P_1(y) = <I(y)>, \tag{3.11}$$

$$P_2(y_1, y_2) = <I(y_1)I(y_2)>, \tag{3.12}$$

where

$$I(y) = |\pi(y)|^2, \tag{3.13}$$

$$<I(y)> = |\pi_{coh}(y)|^2 + \Gamma(y, y), \tag{3.14}$$

and

$$<I(y_1)I(y_2)> = |\pi_{coh}(y_1)|^2|\pi_{coh}(y_2)|^2 + \Gamma(y_1, y_1)\Gamma(y_2, y_2) +$$

$$+ \quad \Gamma(y_1,y_2)\Gamma(y_2,y_1) + 2Re\{\pi(y_1)^*\pi(y_2)\Gamma(y_2,y_1)$$

$$+ \quad \pi(y_2)^*\pi(y_1)\Gamma(y_1,y_2)\}|\pi(y_2)|^2\Gamma(y_1,y_1)$$

$$+ \quad |\pi(y_1)|^2\Gamma(y_2,y_2). \tag{3.15}$$

By using Eq.(3.6) and (3.10), the BEC of Eq.(2.1)) is given by

$$C_{(2)}(y_1,y_2) = \frac{<I(y_1)I(y_2)>}{<I(y_1)><I(y_2)>} \tag{3.16}$$

$$= 1 + 2p(1-p)\gamma(y_1,y_2) + p^2[\gamma(y_1,y_2)]^2. \tag{3.17}$$

However, in the presence of a multiplicity bias, the final expression of Eq.(3.17) needs to be modified.

In order to study the multiplicity bias we need to display explicitly the multiplicity dependence in our QS model. This dependence is discussed in the following section.

3.2 Single domain

To discuss the multiplicity distribution of the pion field, it is necessary to treat the pion field $\pi(y)$ in the above section at the level of second quantization. Here the central problem is to choose an appropriate orthonormal base for the second quantization, and to find the corresponding density operator for a given rapidity domain. This will be done in the subsections below.

3.2.1 Field operator and its P-representation

Giving the correlation function Eq.(3.4), it is most convenient to choose an orthonormal set of wave functions which diagonalize $\gamma(y_1, y_2)$, i.e.,

$$\int \gamma(y, y')\phi_m(y')dy' = \lambda_m \phi_m(y), \qquad m = 1,\ 2,\ ... \tag{3.18}$$

where ϕ_m is the eigenfunction and λ_m is the corresponding eigenvalue. In terms of this base $\{\phi_m\}$, the pion field operator $\pi(y)$ is constructed by its corresponding destruction operator a_m. For the coherent field component, we have

$$\pi_{coh}(y) = e^{-iw_{coh}y} \sum_m a_{coh,m}\phi_m(y). \tag{3.19}$$

The P-representation of the individual m^{th} mode of the coherent component is, therefore, a δ-function, so that

$$\mathcal{P}_{coh,m}(\alpha) = \delta(\alpha - \alpha_{coh,m}), \tag{3.20}$$

where $|\alpha_{coh,m}>$ is given by

$$a_{coh,m}\ |\alpha_{coh,m}> = \alpha_{coh,m}\ |\alpha_{coh,m}>\ . \tag{3.21}$$

Similarly, the corresponding expansion of the chaotic field is written as

$$\begin{aligned} \pi_{chao}(y) &= e^{-iw_{chao}y}\tilde{\pi}(y) \\ &= e^{-iw_{chao}y} \sum_m a_{chao,m}\phi_m(y). \end{aligned} \tag{3.22}$$

The P-representation of the chaotic component (Gaussian ensemble) is

$$\mathcal{P}_{chao,m}(\alpha_{chao,m}) = \frac{1}{\pi\lambda_m} e^{-|\alpha_{chao,m}|^2/\lambda_m}, \tag{3.23}$$

where $|\alpha_{chao,m}>$ is given by

$$a_{chao,m}\ |\alpha_{chao,m}> = \alpha_{chao,m}\ |\alpha_{chao,m}> . \tag{3.24}$$

The above specific assumption of the Gaussian stochasticity also implies that

$$\int d^2\alpha_{chao,m}\ |\alpha_{chao,m}|^{2j}\ \mathcal{P}(\alpha_{chao,m}) = j!\ \lambda_m^2. \tag{3.25}$$

Eq.(3.25) is the key relationship that allows the multi-particle correlation functions of the chaotic filed $\pi_{chao}(y)$ to be factorized into the products of the two-particle field correlation functions Eq.(3.6)[16]. Eq.(3.25) also connects our QS formalism to the traditional formalism in QO as we shall discuss later on. The above pion field $\pi(y)$ can be equivalently represented by

$$\mathcal{P}(\{\alpha_{chao,m}\}) = \prod_m \frac{1}{\pi\lambda_m} e^{-|\alpha_{chao,m}-\alpha_{coh,m}|^2/\lambda_m}, \tag{3.26}$$

which is a displaced Gaussian[6,17].

3.2.2 Multiplicity distributions

In statistical analyses of the convolution of independent distributions, cumulant moments are the most convenient statistical quantity. We shall start with the

factorial moment-generating function $G(s)$ and the factorial cumulant moment-generating function $H(s)$ of a multiplicity distribution $P(n)$ given by[18]

$$G(s) = \sum_{n=0}^{\infty}(1-s)^n P(n), \tag{3.27}$$

$$H(s) = lnG(s),$$

$$= \sum_{k=1}^{\infty}(-1)^k \mu_k \, s^k/k!. \tag{3.28}$$

From Eq.(3.25) and (3.26), the above factorial cumulant μ_k of the multiplicity distribution $P(n)$ is given as[17]

$$\mu_j = (j-1)!\, \overline{n}_{chao}^{j}\, B_j + j!\, \overline{n}_{chao}^{j-1}\, \overline{n}_{coh}\, \overline{B}_j, \tag{3.29}$$

where

$$B_j = \frac{1}{(\Delta y)^j}\int dy_1 ... \int dy_j \gamma(y_1,y_2)\gamma(y_2,y_3)...\gamma(y_j,y_1), \tag{3.30}$$

$$\overline{B}_j = \frac{1}{(\Delta y)^j}\int dy_1 ... \int_d y_j e^{i(w_{coh}-w_{chao})(y_1-y_j)}\gamma(y_1,y_2)$$

$$.\gamma(y_2,y_3)...\gamma(y_{j-1},y_j)$$

$$= \frac{1}{(\Delta y)^j}\int dy_1 ... \int_d y_j \gamma(y_1,y_2)\gamma(y_2,y_3)...\gamma(y_{j-1},y_j). \tag{3.31}$$

The explicit expression for $P(n)$ is, however, still difficult to obtain. This difficulty can be overcome by comparing the Eq.(3.29) with a quantum optical approach, where both the multiplicity distribution $P(n)$ and its factorial cumulants are formally given[5,15]. The quantum optical model, which leads to identical cumulants

of Eq.(3.29), gives the multiplicity distribution of the pion field

$$P(n) = \int dW \mathcal{P}(W) \frac{e^{-W} W^n}{n!}. \tag{3.32}$$

Here $\mathcal{P}(W)$ is the probability density of the random variable W, which is an integrated intensity over the rapidity space Δy, i.e.,

$$W = \int dy I(y), \tag{3.33}$$

with

$$I(y) = |\pi(y)|^2,$$

as defined in Eq.(3.13). From Eqs.(3.19) and (3.22), W is simply given by

$$\begin{aligned} W &= \overline{n}_{coh} + \sum_m (|\alpha_{chao,m}|^2 + \alpha_{coh,m}\alpha^*_{chao,m} + \alpha^*_{coh,m}\alpha_{chao,m}) \\ &= \sum_m |\alpha_{chao,m} + \alpha_{coh,m}|^2. \end{aligned} \tag{3.34}$$

The mean multiplicity of the pion field is now

$$\overline{n} = < W >_{ensemble\ over\ \{\alpha_{chao,m}\}}. \tag{3.35}$$

The above multiplicity distribution Eq.(3.32) shall be generalized to multi-rapidity domains in section 3.3 for the Monte Carlo simulation of BEC in Chapter 4.

3.2.3 Lorentzian profile

As is well known in quantum optics[19], analytical expressions of the multiplicity distribution $P(n)$ are very difficult to obtain in a closed form for finite domains.

The only known exception is the Lorentzian profile with a finite correlation length ξ_y[15,5,17], where

$$\gamma(y_1, y_2) = e^{-|y_1 - y_2|/\xi_y}. \tag{3.36}$$

The above correlation length ξ_y plays an important role when BEC is interpreted. It is related to the radius of the particle production source[6].

In the Monte Carlo calculation of Chapter 4, Eq.(3.36) is used. There are two major reasons. The first is that it is easier for us to test the accuracy of our Monte Carlo calculation. The second is that with a proper choice of the parameter ξ_y, the Lorentzian profile can give a relatively good description of experimental multiplicity data[5].

3.3 Multiple domains

One possible way to discuss the multiplicity dependence of BEC, is to evaluate the joint multiplicity distribution in more than one rapidity domain. The joint probability distribution for finding n_1 particles in a rapidity window $y_1 \leq y \leq y_2$, n_2 particles in a window $y_2 \leq y \leq y_3$, $\cdots$, and n_N particles in the rapidity window $y_N \leq y \leq y_{N+1}$, can be extended in a straight forward way from Eq.(3.32).

For i^{th} bin (see Figure. 3.1 on page 23), $y_i \leq y \leq y_{i+1}$, we have

$$P_i(n_i) = \int dW_i \mathcal{P}(W_i) \frac{e^{-W_i} W_i^{n_i}}{n_i!}, \tag{3.37}$$

with

$$W_i = \int_{y_i}^{y_{i+1}} dy I(y). \tag{3.38}$$

The joint multiplicity distribution is then given as

$$P(\{n_i\}) = \int \cdots \int \prod_i^N \mathcal{P}(\{W_i\}) \frac{(W_i)^{n_i}}{n_i!} e^{-W_i} dW_i. \tag{3.39}$$

Here all the W_i are calculated from the same base of Eq.(3.18) and therefore highly correlated. However, Eq.(3.39) is extremely difficult to evaluate analytically. It is therefore most natural to employ the Monte Carlo simulation to study the Bose-Einstein correlation with a multiplicity bias. In the next chapter, we shall focus on the details of the Monte Carlo procedure and its numerical results.

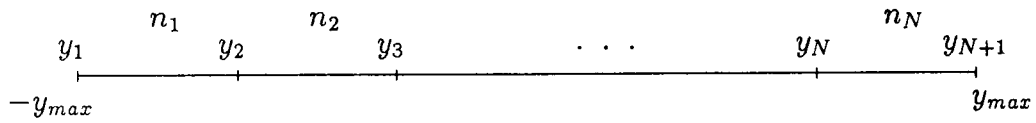


Figure 3.1: Multi domains in rapidity

CHAPTER 4

Monte Carlo Simulation

4.1 Monte Carlo formalism

In the following Monte Carlo simulations, we will calculate $C_{(2)}(y_1, y_2)$ of the Bose-Einstein correlation with and without overall multiplicity bias in the rapidity space $-y_{max} \leq y \leq y_{max}$. In the absence of the multiplicity bias, $C_{(2)}(y_1, y_2)$ is given in Eq.(3.16), that is

$$\begin{aligned} C_{(2)}(y_1, y_2) &= \frac{P_2(y_1, y_2)}{P_1(y_1)P_1(y_2)} \\ &= \frac{< I(y_1)I(y_2) >}{< I(y_1) > \ < I(y_2) >}. \end{aligned} \tag{4.1}$$

Similarly, for a fixed multiplicity n, the intensity correlation is given by

$$\begin{aligned} C^{(n)}_{(2)}(y_1, y_2) &= \frac{P^{(n)}_2(y_1, y_2)}{P^{(n)}_1(y_1)P^{(n)}_1(y_2)} \\ &= \frac{< I(y_1)I(y_2) >^{(n)}}{< I(y_1) >^{(n)} < I(y_2) >^{(n)}}. \end{aligned} \tag{4.2}$$

The numerical calculations of Eqs.(4.1) and (4.2) are performed by dividing the rapidity domain (i.e. $-y_{max} \leq y \leq y_{max}$) into five bins (see Figure. 4.1 on page 25).

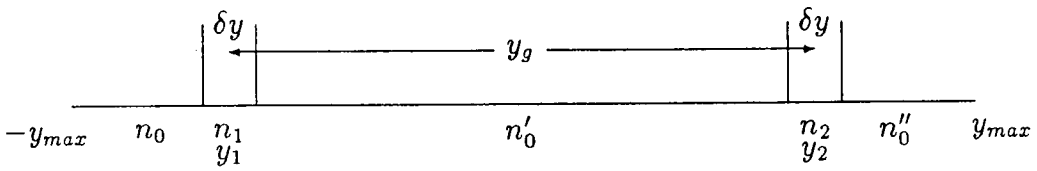


Figure 4.1: Five domains in rapidity

Two small rapidity windows of width δy are centered at y_1 and y_2 with a gap of y_g in between. As the rapidity window width δy approaches to zero, we get

$$\begin{aligned} C_{(2)}(y_1,y_2) &= \lim_{\delta y\to\ 0} \frac{\overline{n_1 n_2}}{(\delta y)^2} [\frac{\overline{n}_1}{\delta y}\frac{\overline{n}_2}{\delta y}]^{-1} \\ &= \lim_{\delta y\to\ 0} \frac{\overline{n_1 n_2}}{\overline{n}_1 \overline{n}_2}, \end{aligned} \tag{4.3}$$

$$\begin{aligned} C^{(n)}_{(2)}(y_1,y_2) &= \lim_{\delta y\to\ 0} \frac{\overline{n_1 n_2}^{(n)}}{(\delta y)^2} [\frac{\overline{n}^{(n)}_1}{\delta y}\frac{\overline{n}^{(n)}_2}{\delta y}]^{-1} \\ &= \lim_{\delta y\to\ 0} \frac{\overline{n_1 n_2}^{(n)}}{\overline{n}^{(n)}_1 \overline{n}^{(n)}_2}, \end{aligned} \tag{4.4}$$

where

$$\overline{n}_j = \int_{y_j-\delta y/2}^{y_j+\delta y/2} <I(y)>\, dy, \quad j=1,2 \tag{4.5}$$

$$\overline{n_1 n_2} = \int_{y_1-\delta y/2}^{y_1+\delta y/2} dy \int_{y_2-\delta y/2}^{y_2+\delta y/2} dy' <I(y)I(y')>\,. \tag{4.6}$$

Because of the multiplicity bias, no analytical expressions for $\overline{n_1 n_2}^{(n)}$ and $\overline{n}^{(n)}_j$ exist. They can only be calculated by Monte Carlo simulation with the constraints

$$n = n_0 + n_1 + n_0' + n_2 + n_0'', \quad n_{min} \le n \le n_{max}. \tag{4.7}$$

Here n_0, n_0' and n_0'' are the number of particles in the rapidity windows $y < (y_1 - \delta y/2), (y_1 + \delta y/2) < y < (y_2 - \delta y/2)$ and $y > (y_2 + \delta y/2)$, respectively, as illustrated in Figure 4.1.

As we already know that, if there is no multiplicity bias, one gets from Eq.(3.17),

$$C_{(2)}(y_1,y_2) = 1 + 2p(1-p)e^{-|y_1-y_2|/\xi_y} + p^2 e^{-2|y_1-y_2|/\xi_y} \tag{4.8}$$

$$= C_{(2)}(y_g), \quad y_g = |y_1 - y_2|, \tag{4.9}$$

where p is the chaoticity, defined by Eq.(3.10), and ξ_y is the two-body correlation length in rapidity space (cf. Eq.(3.36)). For finite values of δy there is a correction term to $C_{(2)}(y_1, y_2)$ so that

$$C_{(2)}(y_1, y_2; \delta y) = C_{(2)}(y_1, y_2) + f(y_1, y_2; \delta y). \tag{4.10}$$

For the leading order of δy,

$$f(y_1, y_2; \delta y) = [\frac{2p(1-p)}{3} e^{-y_g/\xi_y} + \frac{4p^2}{3} e^{-2y_g/\xi_y}](\frac{\delta y}{2\xi_y})^2. \tag{4.11}$$

We are now in a position to estimate specifically $C_{(2)}$ and $C_{(2)}^{(n)}$ of Eqs.(4.3) and (4.4) through Eqs.(4.5) to (4.7).

4.2 Numerical results

Our Monte Carlo simulation is performed with the 60 largest eigenvalues for a Lorentzian profile (Eq.(3.36)). The specific eigenvalues $\{\lambda_m\}$ and eigenfunctions $\{\phi_m\}$ of Eq.(3.18) are given in Appendix A[5]. A flow chart of the Monte Carlo program is shown in Appendix B. The results of this Monte Carlo calculation are given in Figure 4.2, 4.3 and 4.4 on page 28, 29 and 30, respectively. In our calculation, the error of the Monte Carlo results is estimated less than 5%.

Figure 4.2a is a comparison of $C_{(2)}$ as a function of $y_g = |y_1 - y_2|$ between the Monte Carlo simulations without any multiplicity bias (data points), and the

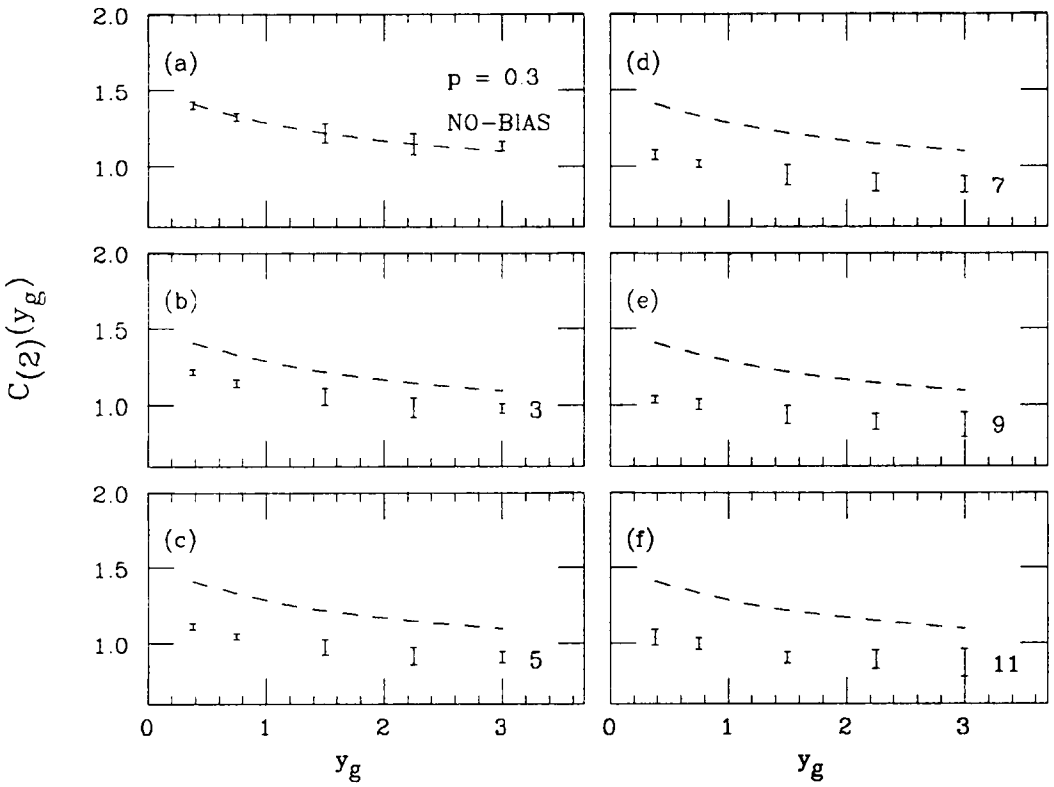


Figure 4.2: Comparison of $C_{(2)}$ for the partially coherent case, between the analytical result of the unbiased formulation Eq.(4.8) (successive dashed curves), and the Monte Carlo simulations without any multiplicity bias (data point), and with fixed n_{min} (value of n_{min} labeled, $n_{max} = \infty$). Parameters used: $p = 0.3$, $\xi = 2.0$, and $< n >= 5$ for $|y| \leq 3.5$, total number of events = 160000.

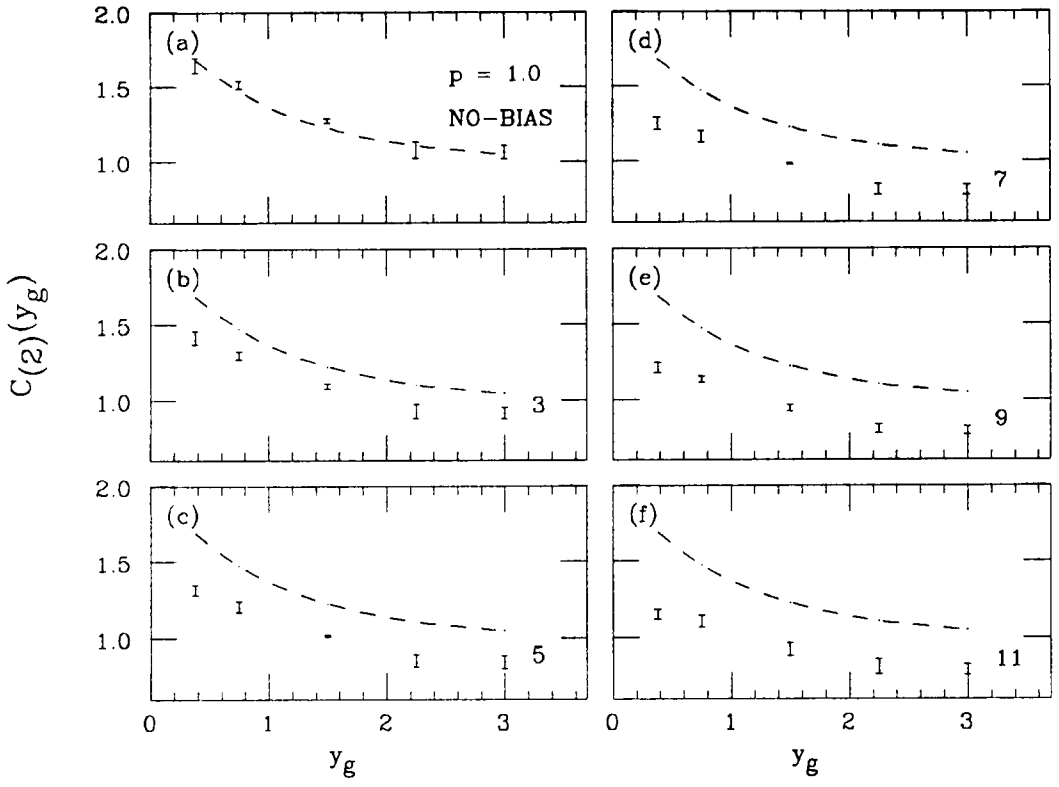


Figure 4.3: Comparison of $C_{(2)}$ for the fully chaotic case. The parameters used are the same as in Figure 4.2, except that the value of chaoticity p is taken as 1.

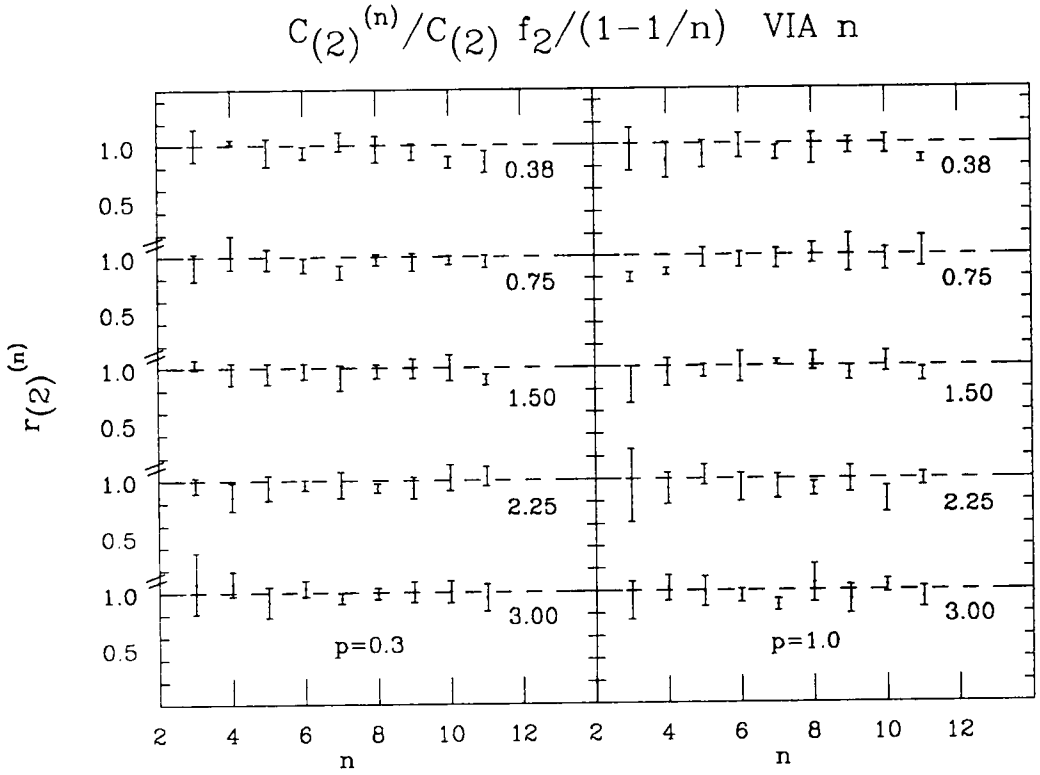


Figure 4.4: Multiplicity dependence of $C_{(2)}$. $r_{(2)}^{(n)}(y_g) = C_{(2)}^{(n)}(y_g)/[C_{(2)}(y_g) f_2 \frac{n-1}{n}]$ is a function of n with a given y_g (labeled by the value of y_g). The parameters are the same as those in Figure 4.2 and Figure 4.3. The dashed line above each dashed curve corresponds to the limiting ratio of 1. Curves on the left side are associated with $p = 0.3$, with $f_2 = 1.20$ and curves on the right side are associated with the fully chaotic limit of $p = 1.0$, with $f_2 = 1.24$.

anticipated analytical results of Eq.(4.8) (dashed curve) for the parameters:

$$p = 0.3 \quad (chaoticity),$$

$$\xi_y = 2.0,$$

$$\overline{n} = 5,$$

$$y_{max} = 3.5.$$

Only five values of y_g are used, which are 0.38, 0.75, 1.50, 2.25 and 3.0. The uncertainties are estimated by the variance among four Monte Carlo samples of 40000 events each. In Figure 4.2b to Figure 4.2f, we compare again $C_{(2)}$ as a function of y_g for a given n_{min} (n_{min} = 3, 5, 7, 9, and 11, respectively, from Figure 4.2b to 4.2f) and $n_{max} = \infty$, (data points) with the anticipated analytical results of Eq.(4.8) (dashed curve) for the same parameters as in Figure 4.2a. It is clear that the overall y_g dependence of the biased $C_{(2)}^{(n)}$, as well as its intercepts, is different from the unbiased solutions.

In order to see the $C_{(2)}$ and $C_{(2)}^{(n)}$ dependences on chaoticity p, another Monte Carlo calculation is carried out with the same parameters as used in Figure 4.3 except that the chaoticity p is taken as 1.0. The results are shown from Figure 4.3a to 4.3f. The systematic influence of n_{min} is seen for both choices of the chaoticity parameter. The same type of behavior is expected for other choices of the average multiplicity $\overline{n}$, and this is confirmed by a Monte Carlo simulation with a choice of

$\overline{n} = 10$.

We have also computed $C_{(2)}^{(n)}$ as a function of y_g for different values of the fixed overall multiplicity n over the whole rapidity window within the same Monte Carlo simulation of Figure 4.2 and 4.3. The resultant distributions thus obtained as a function of the rapidity y_g are similar to the curves in Figure 4.2 and Figure 4.3, but with somewhat different shapes. Moreover, the ratio between $C_{(2)}^{(n)}$ and the unbiased $C_{(2)}$ is empirically observed to be roughly a constant with the inherent errors of the Monte Carlo procedure. We observe that the $C_{(2)}^{(n)}(y_g)$ can be approximated by

$$C_{(2)}^{(n)}(y_g) \approx C_{(2)}(y_g)\frac{n-1}{nf_2}, \tag{4.12}$$

where $f_2 = \overline{n(n-1)}/\overline{n}^2$ is the reduced factorial moment. The results of $C_{(2)}^{(n)}(y_g)$ are also, in general, similar to the earlier data[13], where the values of $C_{(2)}^{(n)} + \frac{1}{n}$ were given (except for the cases of very large n and small y_g). Since both the Monte Carlo estimates of $C_{(2)}^{(n)}$ and the analogous experimental data have fairly large relative errors (due to statistics) and since the theoretical inputs used here are oversimplified (see below for discussion), a more comprehensive chi-square analysis for the determination of the best values of the correlation length ξ_y and chaoticity p in the earlier data[13] was not deemed useful at this stage. We see that the choice of fixing the overall multiplicity n always leads to an antibunching effect superimposed on the traditional BEC effect.

In Figure 4.4, we present the ratio

$$r_{(2)}^{(n)}(y_g) = C_{(2)}^{(n)}(y_g)[C_{(2)}(y_g)\frac{n-1}{nf_2}]^{-1} \tag{4.13}$$

as a function of n with a fixed y_g with $f_2 = 1.20$ for $p = 0.3$; and $f_2 = 1.24$ for $p = 1.0$. It is striking that the ratio $r_{(2)}^{(n)}(y_g)$ thus calculated is quite consistent with unity. For a substantial range of y_g, $C_{(2)}^{(n)}(y_g)$ lies below $C_{(2)}(y_g)$. A strong antibunching effect is therefore present. This is similar but different from the antibunching effect well known in quantum optics[20]. The above expression also indicates that the y_g dependence is the same as that of the unbiased intensity correlation, except for the overall normalization factor. However, the uncertainties in the individual $C_{(2)}^{(n)}(y_g)$ and the fact that we ignore the off diagonal elements of the density matrix ρ prevent us from using the approximate expression of $C_{(2)}^{(n)}(y_g)$ to derive a specific expression for the $C_{(2)}$ with n_{min} taken into account. As a matter of fact, the Monte Carlo simulation shows that $C_{(2)}$ at fixed n_{min} has a modified y_g dependence as compared with $C_{(2)}^{(n)}$.

4.3 Conclusions

$C_{(2)}$ decreases noticeably with n_{min}, and this effect is more pronounced the larger n_{min} is, and the smaller y_g is. Since $C_{(2)}$ for a certain n_{min} cut takes a value less than 1, any expression which is bounded below 1.0 (such as the two

exponential formulae of Eq.(4.8)) is not applicable to the analysis of the inherent correlation length ξ_y and chaoticity p. We might attempt to by-pass this difficulty by the displacement of the base line of $C_{(2)}$, e.g., using $C_{(2)} - C_{(2)}(y_g = 3.5)$. It is, however, easy to see that both the correlation length ξ_y and the intercept would be different. Our Monte Carlo simulation indicates that with $n_{min} \neq 0$ one underestimates the BEC.

The correlation functions $C_{(2)}^{(n)}$ at a fixed value of $y_g = |y_1 - y_2|$ are always smaller than the corresponding unbiased $C_{(2)}$ at the same y_g, thus showing a strong antibunching effect in conjunction with the traditional BEC effect. They are all only mildly increasing with n, in qualitative agreement with the experimental observations[13]. A comparison of this effect with other data[12] is hampered by the fact that the measurements were done as a function of Q^2 (four momentum transfer squared) rather than of $|y_1 - y_2|$, where our formalism applies. It is also hampered by the fact that many experiments were done with reference samples that most likely have different intrinsic multiplicity biases. The overall effect can be rather sensitive to the specific methodology used in individual investigations. For example, the recent UA1 experiment imposed a multiplicity bias on the charged total multiplicity n_{ch}. The resultant bias on the BEC effects includes the effect of charge correlations, and further complicates the issue.

The calculations reported above are approximate for the following reasons,

among others:

- The $\vec{q}_T$ dependence of $C_{(2)}$ is not taken into account.
- They are based on the assumption that the BEC are "stationary" in rapidity y_g, i.e., the many-particle correlations are independent of an overall boost in rapidity.
- The boost values ω_{coh} and ω_{chao} are taken to be equal.

However, we believe that these approximations cannot change the essence of the conclusions reached above. It is unlikely that the effect reported here can be used to interpret the entire strong multiplicity dependence of BEC as was reported in an experimental paper[12]. However, these effects are sufficiently significant that the experimental data have to be corrected before any estimations of the values of BEC parameters like radius and chaoticity become meaningful. Then a fortiori before insight into the dynamics of the n dependence of these parameters can be gained.

CHAPTER 5

Summary

By using the coherent state and the P-representation, a quantum statistical model in rapidity space is built to study the Bose-Einstein correlation with multiplicity dependence. Because of the lack of analytical expressions for BEC with multiplicity dependence, a Monte Carlo simulation is carried out. Our Monte Carlo results are consistent with the general trend of the observed BEC with multiplicity dependence[13]. We believe that this is the first time that the multiplicity bias has been calculated quantum mechanically in the BEC study.

The existing experimental information is still scarce, and only a few attempts have been made to explore the systematic dependence of BEC on various experimental parameters, such as the incident energy, the mass of the target and the projectile, the energy dependence of the emitted particles, or, especially, the rapidity difference and the overall multiplicity bias. Also the theoretical inputs used here are oversimplified. Therefore, a rigorous data-fitting with an appropriate choices of the parameter ξ_y and p is not very useful at this stage. However, our Monte Carlo approach can be used as a testing ground for the future experimen-

tal study of BEC, once more theoretical inputs, such as transverse momentum, nonstationarity, and charge correlation, are included in the quantum statistical ensemble. One of our future research efforts will be along this direction.

According to our quantum statistical formalism, the parameters ξ_y and p extracted by fitting experimental data will relate to the size and the coherence of the region of the particle interaction. A dramatic variation of ξ_y or p will indicate possible phase transitions, such as the formation of a new state of matter.

BIBLIOGRAPHY

BIBLIOGRAPHY

[1] R. Hanbury-Brown and R. Q. Twiss, Phil. Mag. 45, (1956) 633; R. Hanbury-Brown and R. Q. Twiss, Nature 178, (1956) 1046; Nature, 178, (1956) 1447; Proc. Roy. Soc. A242, (1957) 300; Proc. Roy. Soc. A243, (1957) 291.

[2] G. Goldhaber et al., Phys. Rev. 120, (1960) 300.

[3] D. H. Boal et al., Rev. Mod. Phys. 62, (1990) 553.

[4] W. A. Zajc, Columbia University Preprint, Nevis R#1384, Nov., 1987.

[5] C. C. Shih, Phys. Rev. D42, (1990) 3025.

[6] R. M. Weiner, Phys. Lett. B232, (1989) 278.

[7] G. N. Fowler and R. M. Weiner, Phys. Rev. D17, (1978) 3118

[8] M. Gyulassy et al., Phys. Rev. C20, (1979) 2267.

[9] J. C. Botke et al., Phys. Rev. D9, (1974) 813.

[10] R. J. Glauber, Phys. Rev. 131, (1963) 2766.

[11] E. C. G. Sudarshan, Phy. Rev. Lett. 10, (1963) 277.

[12] UA1 Coll., C. Albajar et. al., Phys. Lett. B226 (1989) 410.

[13] N. N. Biswas, et al. Phys. Rev. Lett. 35, (1975) 1059; 37, (1976) 175.

[14] B. Durand et al., Phys. Rev. D13, (1976) 99.

[15] A.K.Jaiswal and C.L.Mehta, Phys. Rev. A2, (1970) 168.

[16] C. C. Shih, Phys. Rev. A40, (1989) 1456.

[17] C. C. Shih, to be published in Phys. Lett. B.

[18] P. Carruthers and C.C. Shih, J. Modern Phys. A2, (1987) 1447.

[19] B. Saleh, Photoelectron Statistics, Springer, Berlin, 1978.

[20] M. Schubert and B. W. Wilhelmi, Nonlinear Optics and Quantum Electronics, Wiley and Sons, N.Y. (1986).

[21] M. Fincke-Keeler, Ph.D. Thesis, University of Bonn, West Germany, 1981.

APPENDIX

APPENDIX A

Eigenvalues and eigenfunctions

For the Lorentzian profile of the correlation function $\gamma(y_1, y_2)$, we have the following integral equation to solve[19],

$$\int_{-y_{max}}^{y_{max}} e^{-|y-y'|/\xi_y} \phi_m(y')dy' = \lambda_m \phi_m(y), \tag{A1}$$

to give the eigenvalue λ_m and the eigenfunction $\phi_m(y)$. The above integral equation can easily be transformed into a standard second order differential equation. Taking a first and second order derivative with respect to y on both sides of Eq.(A1), we get that

$$-\frac{1}{\xi_y}\int_{-y_{max}}^{y} e^{-(y-y')/\xi_y}\phi_m(y')dy' + \frac{1}{\xi_y}\int_{y}^{y_{max}} e^{-(y'-y)/\xi_y}\phi_m(y')dy' = \lambda_m \phi'_m(y), \tag{A2}$$

and

$$\frac{1}{\xi_y^2}\int_{-y_{max}}^{y_{max}} e^{-|y-y'|/\xi_y}\phi_m(y')dy' - \frac{2}{\xi_y}\phi_m(y) = \lambda_m \phi''_m(y), \tag{A3}$$

where $\phi'_m = \frac{d\phi_m}{dy}$, and $\phi''_m = \frac{d^2\phi_m}{dy^2}$. From Eq.(A1), Eq.(A3) can be reduced as

$$(\frac{1}{\xi_y^2} - \frac{2}{\xi_y})\phi_m(y) = \lambda_m \phi''_m(y),$$

i.e.,

$$\phi''_m + w_m^2 \phi_m = 0, \tag{A4}$$

where

$$w_m^2 = \frac{2 - \lambda_m/\xi_y}{\xi_y \lambda_m}, \tag{A5}$$

or

$$\lambda_m = \frac{2/\xi_y}{w_m^2 + 1/\xi_y}. \tag{A6}$$

Comparing Eq.(A1) with Eq.(A4), we see that the integral equation has been converted into a standard second order differential equation Eq.(A4).

The general solution of the above differential equation Eq.(A4) is

$$\phi_m = A_m e^{iw_m y} + B_m e^{-iw_m y}. \tag{A7}$$

By inserting Eq.(A7) into Eq.(A1), with some algebra manipulations, we have

$$\frac{A_m}{1/\xi_y + iw_m} e^{-(1/\xi_y + iw_m)y_{max}} + \frac{B_m}{1/\xi_y - iw_m} e^{-(1/\xi_y - iw_m)y_{max}} = 0, \tag{A8}$$

$$\frac{A_m}{-1/\xi_y + iw_m} e^{(-1/\xi_y + iw_m)y_{max}} + \frac{B_m}{-1/\xi_y - iw_m} e^{(-1/\xi_y - iw_m)y_{max}} = 0. \tag{A9}$$

The eigenvalues $\{\lambda_m\}$ (Eq.(A6)) are given by the following two equations,

$$\frac{1}{\xi_y} + w_m \, cot(w_m y_{max}) = 0, \tag{A10}$$

and

$$\frac{1}{\xi_y} - w_m tan(w_m y_{max}) = 0. \tag{A11}$$

Here λ_m is calculated numerically for our Monte Carlo program. Given the eigenvalue λ_m, the coefficients A_m and B_m of Eq.(A7) are determined by the normal-

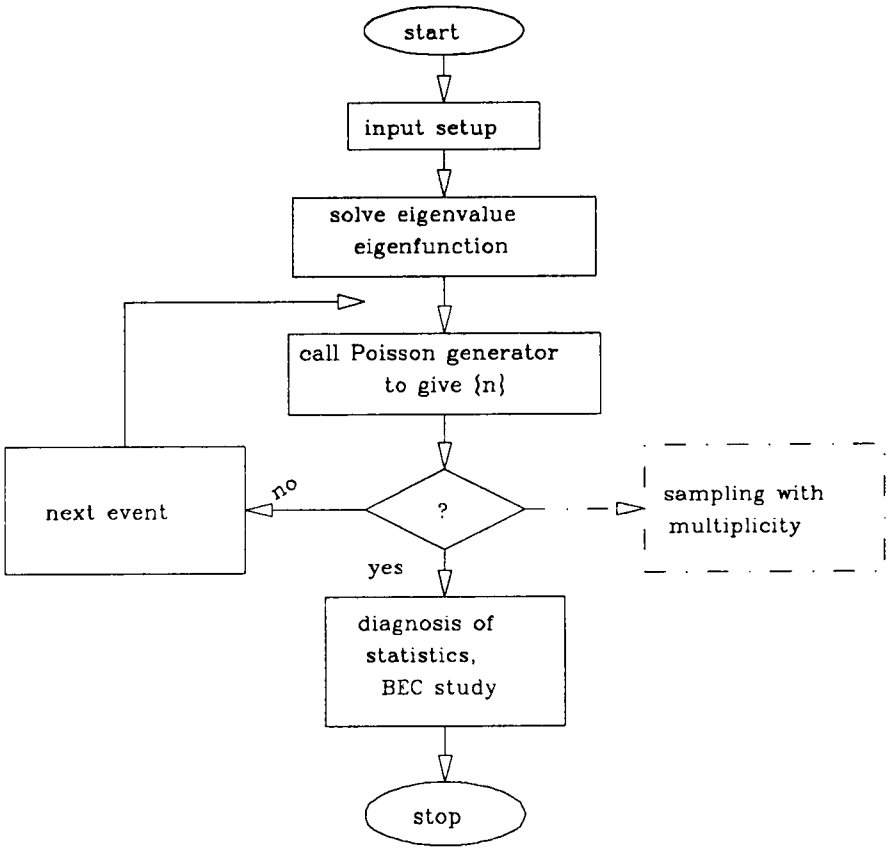
ization condition,

$$\int_{-y_{max}}^{y_{max}} |\phi_m(y)|^2 dy = 1. \tag{A12}$$

In order to have an economic Monte Carlo calculation, a few words are necessary about how many eigenvalues $\{\lambda_m\}$ and eigenfunctions $\{\phi_m\}$ should be used. Theoretically, the more eigenvalues chosen, the less the truncation error will be. Since it is impossible to choose an infinite number of eigenvalues, we have to sacrifice the accuracy of Monte Carlo results in order to have relatively reasonable computer CPU time. The number of eigenvalues is fine-tuned in our calculation to give a less than 5% error with a reasonable computer CPU time. It should be added that this choice of the number of eigenvalues depends on the input parameters, chaoticity p, average multiplicity $\overline{n}$, the correlation length ξ_y and the rapidity window under considerations.

APPENDIX B

Monte Carlo flow chart



VITA

Xiaochun He (賀小春) was born in Jiaxian, Shaanxi, P. R. China on Jan. 28, 1963. According to Chinese customs, being born in that year he is a "rabbit". He started his elementary school education at age six and attended a university at age seventeen. He received a Bachelor of Science degree in Physics from the North-West University, Xian, Shaanxi, P. R. China, in 1984. After studying theoretical nuclear physics for two years at the Institute of Modern Physics in Lanzhou, Gansu, P. R. China, he came to America to study for a Ph.D. in Physics at the University of Tennessee in 1986. During this period, he followed his instructor, Prof. C. C. Shih, to West Germany for six months doing research in the Department of Physics, University of Marburg. He and his instructor have jointly published four papers in his four and half years study. This dissertation is mainly concentrated on one of their published papers. He will receive a Ph.D. in May, 1991.

Studying Physics has been one of his most favorite things to do. It makes his life reliable and stable, it also makes him more "stupid" which he likes very much. His limited hobbies are arts and sports.